# High-Frequency Surface Acoustic Waves Excited on Thin-Oriented $LiNbO_3$ Single-Crystal Layers Transferred Onto Silicon

Thomas Pastureaud, Marc Solal, *Member, IEEE*, Béatrice Biasse, Bernard Aspar, Jean-Bernard Briot, William Daniau, William Steichen, Raphaël Lardat, Vincent Laude, *Member, IEEE*, Alain Laëns, Jean-Michel Friedt, and Sylvain Ballandras

***Abstract*—The need for high-frequency, wide-band filters has instigated many developments based on combining thin piezoelectric films and high acoustic velocity materials (sapphire, diamond-like carbon, silicon, etc.) to ease the manufacture of devices operating above 2 GHz. In the present work, a technological process has been developed to achieve thin-oriented, single-crystal lithium niobate ($LiNbO_3$) layers deposited on (100) silicon wafers for the fabrication of radio-frequency (RF) surface acoustic wave (SAW) devices. The use of such oriented thin films is expected to favor large coupling coefficients together with a good control of the layer properties, enabling one to chose the best combination of layer orientation to optimize the device. A theoretical analysis of the elastic wave assumed to propagate on such a combination of material is first exposed. Technological aspects then are described briefly. Experimental results are presented and compared to the state of art.**

## I. Introduction

Because the early developments of surface acoustic wave (SAW) devices [1], many advances have been achieved to answer the continuous demand for components (filters, resonators) exhibiting improved properties (low losses, large bandwidth, strong rejection, high-spectral purity, etc.). These improvements were required because of the increased capabilities of electronic systems integrating these passive devices to handle more and more data with enhanced information flows. Particularly in the telecommunication domain, the researchers and engineers must provide a significant effort to innovate and answer the demand for high-frequency, wide-band filters.

Manuscript received April 3, 2006; accepted October 27, 2006. This work was partly supported by the French National Network for Research in Communication (RNRT) as the OASIS project under grant #98 S 0324.

T. Pastureaud, W. Steichen, J.-B. Briot, R. Lardat, and A. Laëns are with TEMEX, F-06904 Sophia-Antipolis Cedex, France.

M. Solal is with SAWTEK Inc., Orlando, FL.

B. Biasse is with the Comissariat à l'Energie Atomique (CEA)-DRT—Laboratoire d'Electronique et de Traitement de l'Information F-38054 Grenoble Cedex 9, France.

B. Aspar is CEO of TRACIT, Grenoble, France.

J.-M. Friedt is with SENSEOR, F-06904 Sophia-Antipolis Cedex, France.

W. Daniau, V. Laude, and S. Ballandras are with the Institut FEMTO-ST, UMR CNRS 6174, UFC-ENSMM-UTBM, F-25044 Besançon Cedex, France (e-mail: ballandr@femto-st.fr).

Digital Object Identifier 10.1109/TUFFC.2007.321

In this context, a lot of work has been devoted to the fabrication of radio-frequency (RF) passive devices built on layered substrates, taking advantage of the combination of piezoelectric layers and high acoustic velocity materials like sapphire, carbon-diamond thick layers or silicon [1], [2]. Those piezoelectric layers generally are obtained using sputtering or various chemical vapor deposition techniques, generally providing C-oriented films with moderately controlled piezoelectric properties. Furthermore, most of these deposition techniques requires specific substrate orientations, or at least buffer layers (for instance platinum, titanium, etc.) for lattice matching reasons.

Many results have been published concerning AlN, ZnO or even lithium niobate ($LiNbO_3$) layers on the abovementioned substrates, and some advances have been reported on crystal orientation control these very last years [3]–[5]. However, surface wave devices built along this approach poorly fit the RF filter requirements in terms of electromechanical coupling (always smaller than 5%), propagation losses and frequency stability simultaneously.

Especially for $LiNbO_3$ (but also for most of the highly coupled piezoelectric materials), the deposition of C-oriented layers does not provide the best configuration for the excitation of SAW, yielding coupling coefficients for both Rayleigh and shear polarized waves much smaller than those of SAW propagating on standard, single-crystal cuts as YZ or (YX$l$)/128° $LiNbO_3$ or even (YX$l$)/42° lithium tantalate ($LiTaO_3$).

In this work, we use a layer transfer process invented at Comissariat à l'Energie Atomique-Direction de la Recherche Technologique-Laboratoire d'Electronique et des Technologies de l'Information (CEA-DRT-LETI) based on ion implantation and direct wafer bonding to obtain oriented piezoelectric layers on (100) silicon. The combination of $LiNbO_3$ and silicon is particularly considered for the excitation and propagation of highly coupled shear waves (the most preferred solution for RF applications). In this process, a very good adhesion between $LiNbO_3$ and silicon is achieved, without any intermediate layer. The adhesion force is found to be compatible with acoustic wave guide applications.

In the first section of this article, theoretical predictions of elastic waves excited and guided in the considered structure [i.e., (YX) $LiNbO_3$ on (100) silicon] are reported. The second part of the paper is dedicated to the main tech-

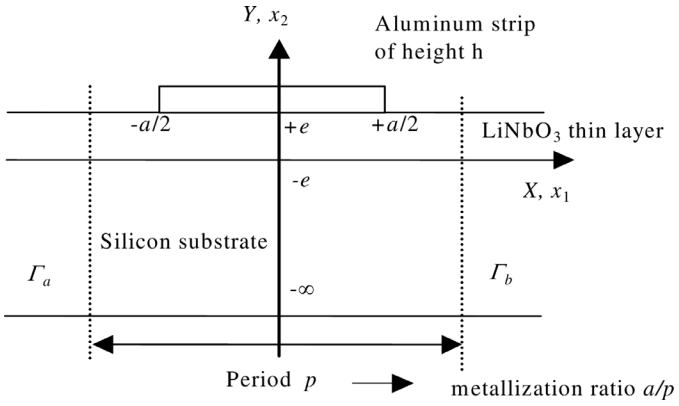


Fig. 1. Scheme of the general geometry of the addressed problem.

nological aspects of the developed process. Experimental measurements of guided elliptic and shear polarized waves on four-inches (YX) $LiNbO_3$/(100) silicon wafers are exposed and compared to theoretical predictions. These measurements have been performed using 1 and 2 GHz single-port resonators allowing for an accurate characterization of the wave-guide in terms of phase velocity, electromechanical coupling, electrode grating reflection, and propagation losses. Some particular properties of the corresponding devices are also reported. Experimental results are discussed regarding theoretical predictions, as well as the best results obtained for SAW devices on silicon-based, layered substrates.

## II. Theoretical Analysis

The analysis of the combination of oriented $LiNbO_3$ (YX) thin layer on (100) silicon takes advantage of all the developments previously presented for layered structures [6]. A stable scattering-matrix method [7] is used to compute the Green's function and the surface permittivity of the multilayer. Included in a mixed finite element/boundary integral Method (FEA/BIM) approach [6], the harmonic admittance then is calculated. Among all standard $LiNbO_3$ crystal orientations [namely, (YX), (YX$l$)/41°, (YX$l$)/64° and (YX$l$)/128° cuts], the (YX) cut was found to be the most interesting solution for shear wave guiding because of its large coupling coefficient and phase velocity. The leaky shear wave on (YX) cut is known to exhibit a strong leakage, expected to be suppressed by the guiding effect. The general geometry of the problem is depicted in Fig. 1. As shown further, elastic wave guides built using thin $LiNbO_3$ layers atop silicon can support Rayleigh-like wave as well as shear wave propagation, the later being particularly considered in this work.

Silicon (100) is particularly well suited for fabricating elastic shear wave guides because transversely polarized bulk acoustic waves exhibits velocity propagation in the vicinity of 5800 m/s, larger than shear polarized leaky-SAWs on any singly rotated $LiNbO_3$. Nevertheless, it also is reasonably low to avoid large acoustic mismatches between the layer and the substrate, yielding a too strong dependence of the wave characteristics (particularly the phase velocity and the electromechanical coupling) on the piezoelectric layer thickness. Three different electrical conditions have been considered at the interface between the $LiNbO_3$ thin layer and the silicon wafer. Silicon is first assumed intrinsic (dielectric) or ideally conductive (metallike), then its actual conductivity is taken into account. This later point is achieved considering the following relations between the electric field $E_i$ and the electrical charge $\rho$ in silicon:

$$\sigma\, div.E + j\omega\rho = 0 \ \text{ and } \ \varepsilon\, div.E = \rho. \tag{1}$$

This relation yields the definition of an effective dielectric constant pointing out the effect of silicon conductivity as an equivalent frequency-dependent source of dielectric losses:

$$\varepsilon_{\text{eff}} = \varepsilon - j\frac{\sigma}{\omega}. \tag{2}$$

These relations can be exploited for both effective permittivity and harmonic admittance approaches that have been used in the present study to predict wave characteristics. The first parameter allows one to first identify the best operating conditions in regard with wave guiding. The second is preferably used to predict actual electrical properties of the guided wave (coupling, velocity, reflection, directivity, losses).

The computations have been performed using the Smith and Welsh data set for $LiNbO_3$ [8], and elastic characteristics of silicon as given in Landolt-Bornstein tables [9]. The results are reported in Fig. 2, showing the evolution of the main characteristics of the second guided mode (shear polarized), extracted from the effective permittivity, versus $LiNbO_3$ thickness considering intrinsic (a) or conductive (b) silicon. In both cases, an optimal frequency-thickness product $f.t$ can be found to take advantage of the largest coupling coefficient [more than 20% in the case of (YX) $LiNbO_3$/(100) intrinsic silicon]. One can easily see that, for a given operating frequency, the optimal $LiNbO_3$ thickness is smaller when using intrinsic silicon rather than conductive silicon. In the frequency range 1–2 GHz, the typical $LiNbO_3$ thickness should be equal to 0.75 $\mu$m for intrinsic silicon, but it should be more than 2 $\mu$m for conductive silicon. However, the velocity dispersion is smaller in the later case than it is for intrinsic silicon-based devices.

The case of partially conducting silicon then is addressed separately. Due to the piezoelectric coupling of $LiNbO_3$, the electrical field associated with the wave excitation and propagation within the piezoelectric layer—and which penetrates into the silicon—is strong enough to generate an electric current within the semiconductor substrate. This later drains a part of the energy of the guided wave, yielding propagation losses. The evolution of these losses, of the electromechanical coupling and the phase velocity versus silicon resistivity is reported in Figs. 3 and 4 for different frequency-thickness products (0.5 and 1 GHz.$\mu$m or km.s$^{-1}$ respectively) close to the

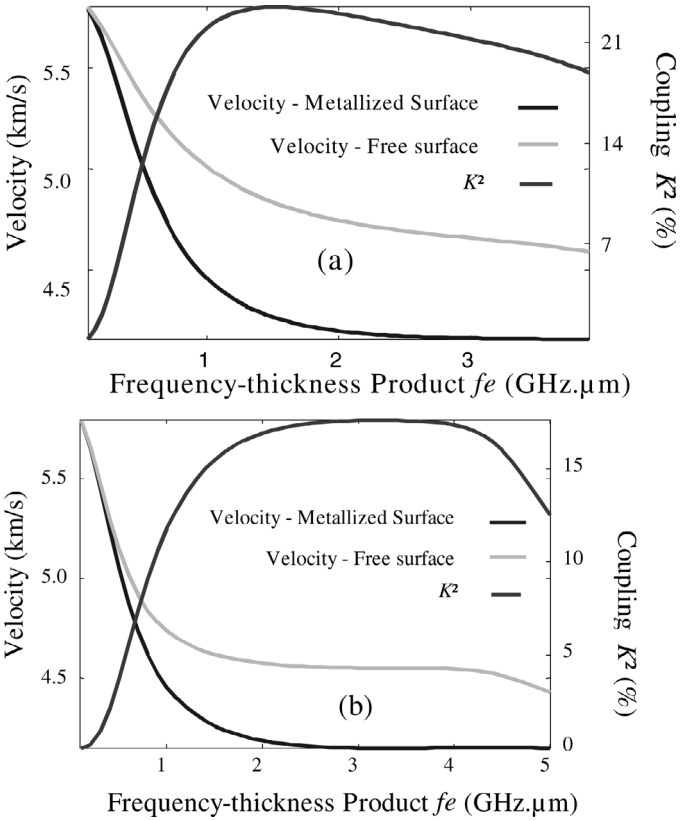


Fig. 2. Velocity and coupling coefficient of shear polarized wave on (YX)$LiNbO_3$/(100) Si (a) intrinsic (b) perfectly conductive, results extracted from effective permittivity.

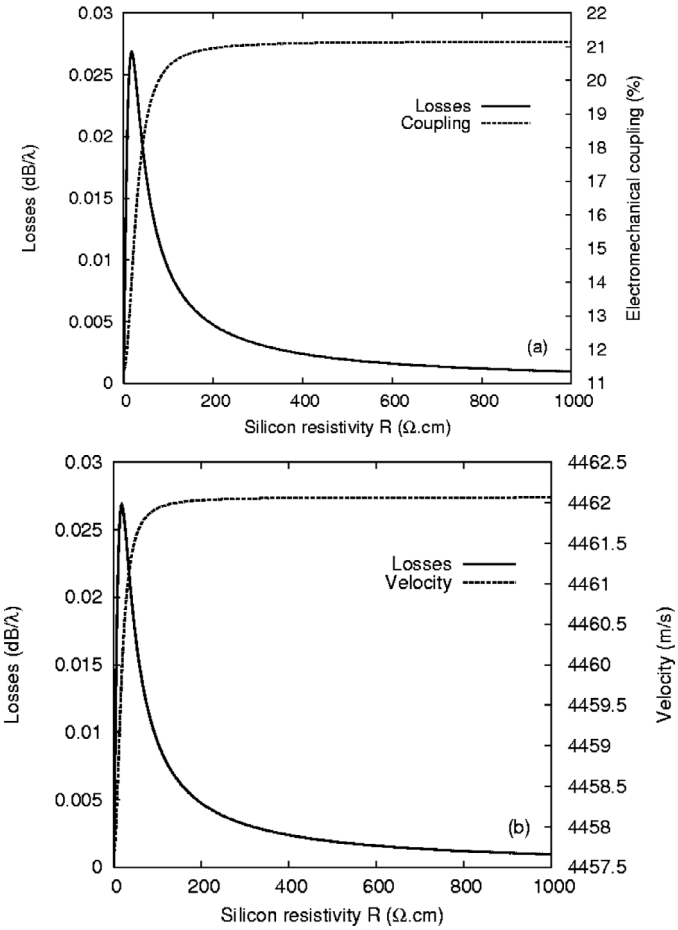


Fig. 3. Evolution of the propagation losses, coupling coefficient and phase velocity versus the silicon resistivity-shear polarized wave on (YX)$LiNbO_3$/(100), $f.t = 1$ GHz.$\mu$m.

ones tested experimentally. One can see that intermediate situations between conductive and intrinsic substrates should be avoided to minimize propagation losses.

In order to try and benefit from the largest accessible coupling factor, and considering technology constraints about $LiNbO_3$ thickness, the combination of high-resistivity silicon (typically 1 k$\Omega$.cm) and (YX) $LiNbO_3$ would be preferred for the fabrication of experimental test devices. Practically, tests were most of the time performed on available standard conductivity silicon wafers (14 $\Omega$.cm). As shown by theoretical predictions, it is not a very favorable working point, but experimental results show that, in such a configuration, the losses due to substrate conductivity are not large enough to prevent either the propagation or the accurate characterization of the mode. The harmonic admittance of the stratified structure [10] also has been computed for these configurations to identify the most important parameters of the wave (velocity, coupling coefficient, propagation losses, reflection coefficient, and directivity) and to compare them to experimental measurements in the next section. We also have computed the sensitivity $S$ of the wave velocity $V$ versus the $LiNbO_3$ thickness $t$, defined as the ratio of the relative velocity change versus the relative error on thickness ($\Delta V/V = S \times \Delta t/t$). Values of 22% and 13% were found for $f.t$ products, respectively, equal to 1 and 2 GHz.$\mu$m. Even if not negligible, one can consider these operating points as moderately sensitive to the $LiNbO_3$ layer thickness.

## III. Experiments

### A. Technological Aspects

The transfer process is mainly based on an ion implantation step followed by a direct wafer bonding [11]. It is comparable to the UNIBOND$^{TM}$ process developed by SOITEC (Grenoble, France). It can be decomposed in four major steps, as shown in Fig. 5:

- Ion implantation is performed in the $LiNbO_3$ wafer. This step induces formation of an in-depth weakened layer.
- The $LiNbO_3$ wafer is bonded to a silicon wafer by direct wafer bonding.
- The splitting step is thermally induced in the weakened layer [see Fig. 6(a)].
- The rough surface left after splitting is removed by soft-touch polishing [see Fig. 6(b)].

This process has been successfully implemented, providing almost perfectly transferred $LiNbO_3$ layer on a 4-inch silicon wafer (see Fig. 7).

Single-port synchronous resonators have been used to characterize the two first modes excited in the compound (YX) $LiNbO_3$/(100) silicon wave guide. The inter-digital

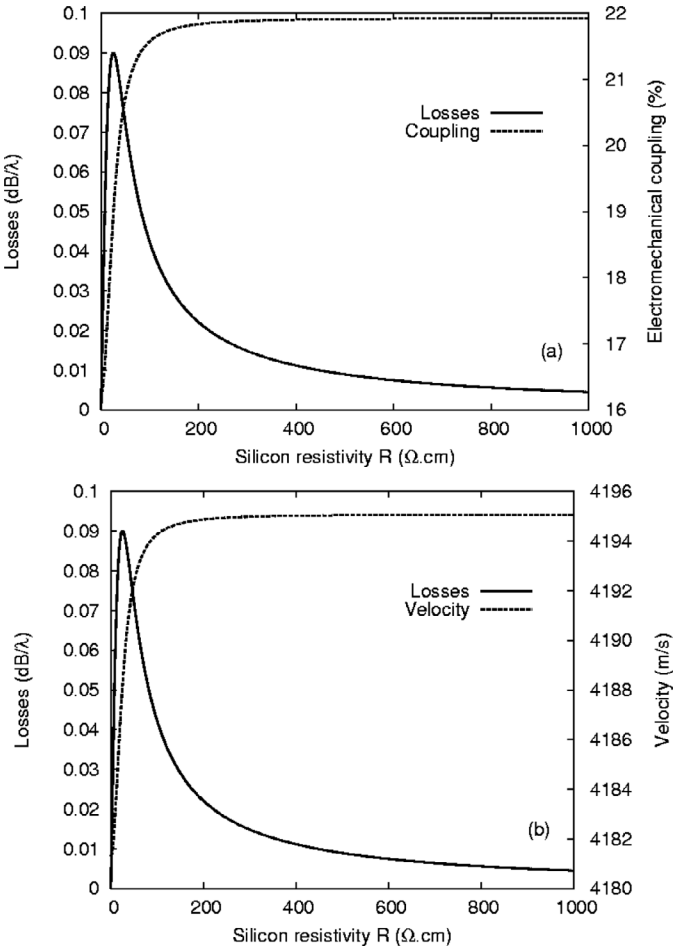


Fig. 4. Evolution of the propagation losses, coupling coefficient, and phase velocity versus the silicon resistivity-shear polarized wave on (YX)$LiNbO_3$/(100), $f.t = 2$ GHz.$\mu$m.

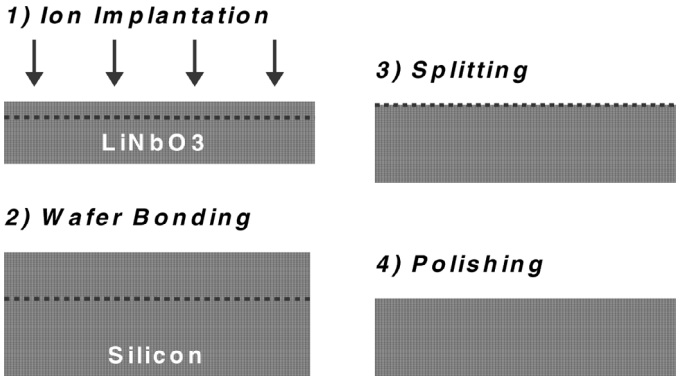


Fig. 5. Principle of the fabrication process of $LiNbO_3$/silicon compounds.

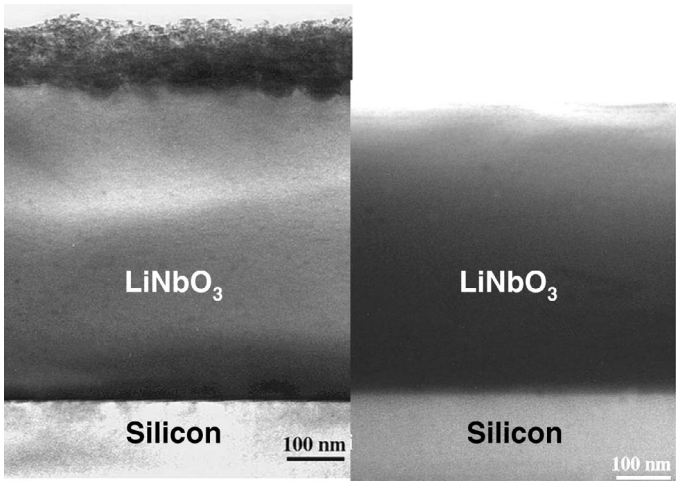


(a) (b)

Fig. 6. XTEM views of the $LiNbO_3$ layer after splitting (a) and touch polishing (b).


Fig. 7. Photo of a 4-in. wafer with almost perfectly transferred Y-cut $LiNbO_3$ top layer.

transducer (IDT) was composed of 100 finger pairs, with 50 strip in the mirror. The grating periods were 2 and 1 $\mu$m (yielding acoustic wavelengths, respectively, equal to 4 and 2 $\mu$m), the electrode height was set to 100 nm ($h/2p = 2.5\%$ and 5%), and the metallization ratio $a/p = 0.5$ at 1 GHz and 0.4, 0.5, and 0.6 at 2 GHz. Different attempts have been performed according to technological advancements, providing a wide set of experimental results.

### *B. Experiments at 1 GHz*

As shown in Fig. 7, the optimization of the process enabled the transfer of a 0.5-$\mu$m thick (YX) $LiNbO_3$ layer on 4-in. silicon wafers (silicon resistivity still about 14 Ω.cm). A first set of experiments has been performed, taking advantage of these wafers compatible with the TEMEX (Sophia Antipolis, France) product line. SAW devices consequently were manufactured using the TEMEX standard process (stepper 5X and dry etching of the Al electrodes). Once the devices achieved, they were tested on a Süss Microtec (Saint-Jeoire, France) RF probe station (Fig. 8), and a fit procedure of the two guided modes using a mixed-matrix model [12] was used to extract the effective propagation parameters from the electrical

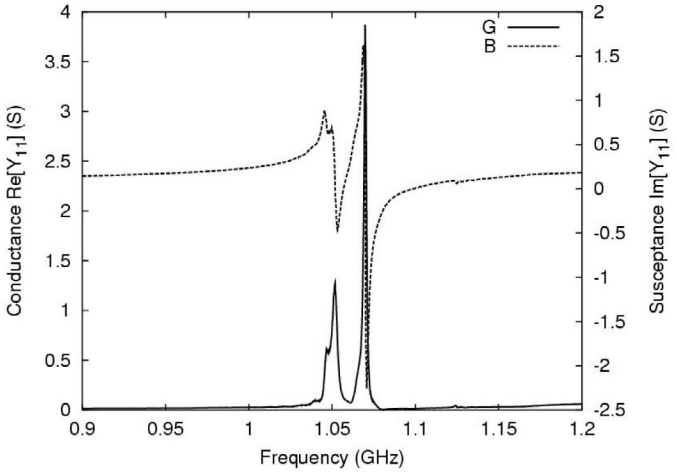


Fig. 8. Admittance of the 1 GHz devices.

measurements. The effective mixed-matrix parameters of the Rayleigh-like mode have been found similar to the theoretical predictions: the wave actually propagates at 4198 m.s$^{-1}$ and exhibits a coupling factor $K_s^2$ of 2.0%. The temperature dependence of the resonator on this mode leads to a first order temperature coefficient of frequency (TCF = −42 ppm/K) very close to what is expected (−38 ppm/K). However, the phase velocity of the shear mode was found significantly different from the theoretical calculations (experimental velocity 4384 m.s$^{-1}$ compared to 4825 m.s$^{-1}$ theoretically predicted) [13]. But the electromechanical coupling coefficient as well as the reflection coefficient are closer to theoretical predictions ($K_s^2 \sim 6\%$ and $|R| \sim 7.7\%$ compared to 7 and 9.3%, respectively). The temperature dependence of the shear mode of the resonator has been measured as well, and leads to a TCF equal to −40 ppm/K, smaller than the theoretical predictions. It should be noted also that, due to variations of silicon conductivity with incident light intensity, photosensitive phenomena also were observed. The best Q-factors were consequently measured with no light sources. All the wave characteristics were found larger than those already obtained with most of the piezoelectric thin films deposited on silicon.

### *C. Experiments at 2 GHz*

As in previous experiments, the tested devices consist of single-port synchronous resonators composed of a 50-finger pair IDT surrounded by two, 50-electrode Bragg mirrors. As described in Section III-A, the mechanical period $p$ was 1 $\mu$m, and an acoustic aperture of 100 $\mu$m was chosen to get rid of any unwanted diffraction effect. Experimental measurements are plotted in Fig. 9. The wave characteristics have been extracted from these measurements and reported in Table I. Harmonic admittance of the device also have been computed, allowing for the characterization of the regarded mode near 2 GHz.

The characteristics have been computed for the nonleaky shear wave, yielding a theoretical velocity of

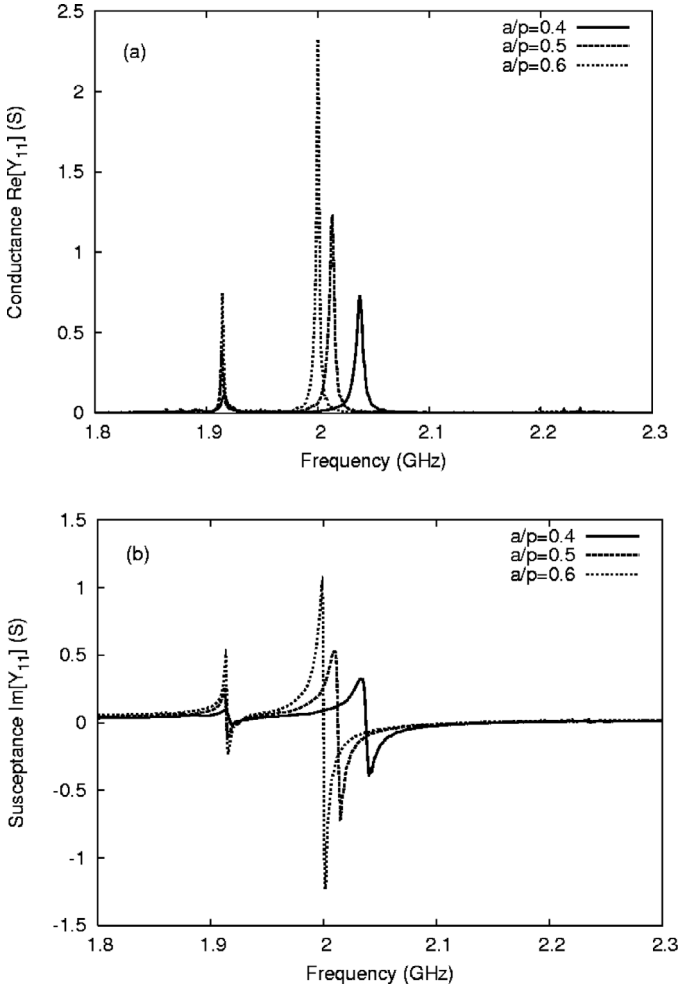


Fig. 9. Admittance of the 2 GHz devices for different metallization ratio (a) conductance (b) susceptance.

4300 m.s$^{-1}$, an electromechanical coupling equal to 14.5% as well as the reflection coefficient. Even if the experimental coupling is slightly smaller than the predicted one, it is shown that the material almost behaves like expected in the sense of electromechanical coupling. The shear mode electromechanical coupling and reflection coefficients are actually doubled when operating at 2 GHz. Also, the Rayleigh-like wave properties change significantly. The coupling clearly decreases whereas the reflection coefficient increases. Considering these new results at 2 GHz ($K_s^2$ equal to 12.5% and 15% for the reflection coefficient), we definitely establish the state-of-the-art of SAW excited in piezoelectric layer/massive substrate wave guides. One also can note that the frequency shift between the three metallization ratios is well predicted [14]. The resonance of the Rayleigh-like wave arises at the end of the frequency stop band (negative reflection coefficient). It is found experimentally and theoretically almost insensitive to the metallization ratio. The discrepancy between theoretical and experimental resonance frequencies can be explained by updating the shear elastic constants of the material. Actually, an improved agreement is obtained when reducing the $C_{44}$ and $C_{55}$ elastic constants (which actually govern

TABLE I
THEORY-EXPERIMENT ASSESSMENT FOR RAYLEIGH AND SHEAR WAVE CHARACTERISTICS ON (YX)$LiNbO_3$/STANDARD RESISTIVITY SILICON FOR A $f.t$ PRODUCT EQUAL TO 0.5 AND 1 GHz.$\mu$m.[1]

| | Velocity (metallized) m.s$^{-1}$ | Coupling coefficient % | Reflectivity % | Thermal sensitivity (TCF1) ppm/K |
|---|---|---|---|---|
| Rayleigh at 1 GHz (theory) $a/p = 0.5$, $h/\lambda = 2.5\%$ | 4163 | 2.15 | 0.39 ($\angle 90°$) | −38 |
| Rayleigh at 1 GHz (experiments) | 4198 | 2.0 | 0.4 ($\angle 90°$) | −42 |
| Rayleigh at 2 GHz (theory) $a/p = 0.6$, $h/\lambda = 5\%$ | 3749 | 1.7 | 2.83 ($\angle 90°$) | −43 |
| Rayleigh at 2 GHz (experiments) | 3777 | 1.3 | 4.2 ($\angle 90°$) | — |
| Shear at 1 GHz (theory) $a/p = 0.5$, $h/\lambda = 2.5\%$ | 4825 | 7.0 | 9.3 | −65 |
| Shear at 1 GHz (experiments) | 4384.5 | 6 | 7.7 ($\angle 0°$) | −40 |
| Shear at 2 GHz (theory) $a/p = 0.6$, $h/\lambda = 5\%$ | 4311 | 15.4 | 15.85 ($\angle 0°$) | −75 |
| Shear at 2 GHz (experiments) | 4200 | 12.5 | 15 ($\angle 0°$) | −50 |

[1]Theoretical data computed using Smith and Welsh's coefficients for $LiNbO_3$ [8].

the shear wave velocity) from 10% of their initial values (55 GPa instead of 59.5 GPa). Because these coefficients influence the Rayleigh wave too, the $C_{66}$ elastic constant also was increased by an amount of 10% of its initial value (80.85 GPa instead of 72.85 GPa), yielding a good matching between theoretical and experimental resonance frequencies. Also, a better agreement is obtained when assuming a smaller silicon resistivity ($\rho = 0.1\,\Omega$.cm) than the one previously considered (14 $\Omega$.cm). The theoretical previsions considering these parameters are reported in Fig. 10.

We also have measured the first order TCF of the nonleaky shear mode. This result is reported in Fig. 11. The previous TCF characterizations, which were performed on small $LiNbO_3$/Si parts, did provide a value of −40 ppm/K (section B), which was twice smaller as expected theoretically. In the set of experiments performed at 2 GHz, the TCF is found in the range of −50 ppm/K (see Fig. 11). Such a value also is quite different from theoretical predictions, and it tends to indicate either that the theoretical assumptions of the TCF calculation do not match the real situation, or that some thermoelastic properties are affected by the bonding process. The second hypothesis is coherent with the fact that discrepancies still persist between theory and experiment concerning the phase velocities of the nonleaky shear guided wave. Table I summarized all the experimental data for the different modes, compared with theoretical predictions.

## IV. CONCLUSIONS

A novel technological process has been developed and successfully tested for the transfer of single-crystal, $LiNbO_3$-oriented layers on (100) silicon. Four-inch wafers have been achieved, allowing the fabrication of SAW devices using industrial techniques. Using a standard conductivity silicon substrate almost behaving like a conduc-

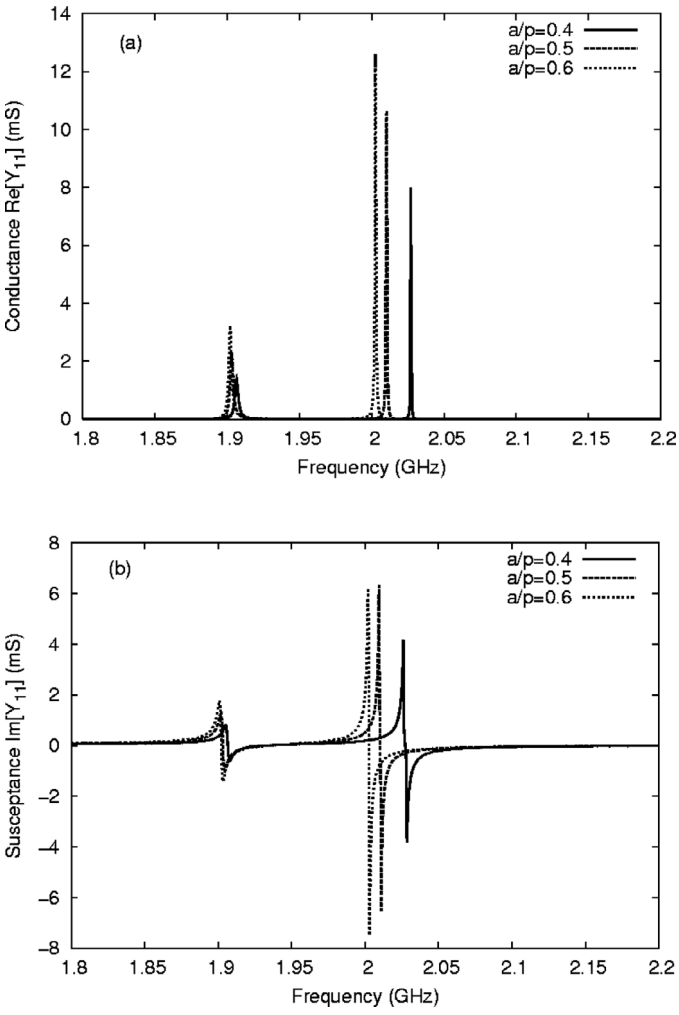


Fig. 10. Theoretical harmonic admittance corresponding to the experimental devices of Fig. 11 after updating the $LiNbO_3$ elastic constant (a) conductance (b) susceptance.

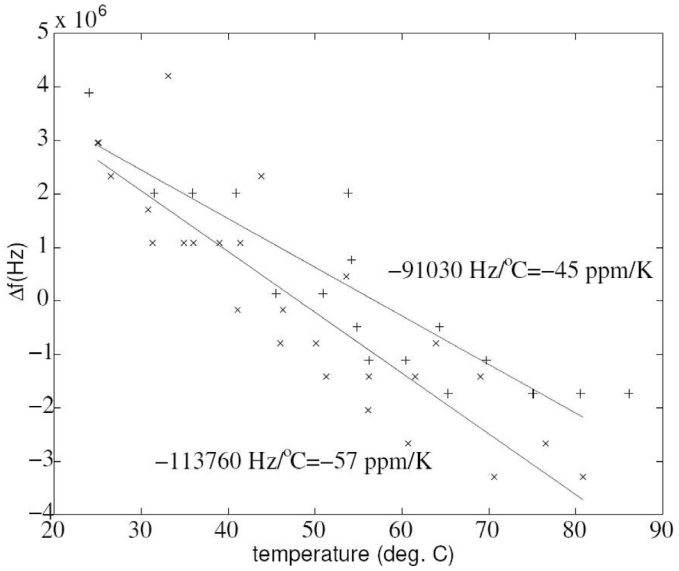


Fig. 11. Temperature coefficients of frequency of the 2 GHz resonators.

tive one, a good agreement is found between theoretically predicted and experimental electromechanical coupling coefficient of the nonleaky shear wave (the second mode of the structure). Two sets of resonators, respectively, operating in the vicinity of 1 and 2 GHz have been fabricated and characterized. The electromechanical coupling coefficient of the nonleaky shear wave is doubled when multiplying the operating frequency by a factor of 2, and a reflection factor equal to 15% has been measured for the 2 GHz resonators. Theoretical predictions of these characteristics are in good agreement with experiments. As a consequence, improving the knowledge of the elastic properties of the compound substrate remains the main difficulty to enable the use of such substrates for real filtering applications. Moreover, as shown theoretically, the tested operating points are far from the optimal one considering conductive silicon, corresponding to a frequency-thickness product equal to 3 GHz.$\mu$m. Consequently, we can expect better results if using thicker niobate layers. Another way to benefit from the optimal operating conditions would consist in reducing the grating period (for instance, a period of 0.2 $\mu$m and a film thickness equal to 0.6 $\mu$m would yield operating frequencies close to 5 GHz). In both cases, technological difficulties have to be overcome, but one should note that the obtained characteristics are quite sufficient to address modern filter requirements, yielding an interest for this above-integrated circuit solution for integrated signal processing devices.

## Acknowledgment

The authors would like to thank Jean-Michel Hodé for his efforts in setting up the project.

## References

[1] D. L. Dreifus, R. J. Higgins, R. B. Henard, R. Almar, and L. P. Solie, "Experimental observation of high velocity pseudo-SAWs in ZnO/diamond/Si multilayers," in *Proc. IEEE Ultrason. Symp.*, 1997, pp. 191–194.

[2] J. Lee, N. Little, T. Rabson, and M. Robert, "Thin-film Lithium niobate on diamond-coated silicon substrates for surface acoustic wave applications," in *Proc. IEEE Ultrason. Symp.*, 1999, pp. 269–272.

[3] F. S. Hickernell, "Thin-film for SAW devices," *Int. J. High Speed Electron. Syst.*, vol. 10, no. 3, pp. 603–652, 2000.

[4] H. Nakahata, A. Hachigo, K. Itakura, S. Fujii, and S. Shikata, "SAW resonators of $SiO_2$/ZnO/diamond structure in GHz range," in *Proc. IEEE Int. Freq. Contr. Symp.*, 2000, pp. 315–319.

[5] Y.-Y. Chen, T.-T. Wu, and T.-T. Chou, "Analysis of the frequency response of a dispersive IDT/ZnO/sapphire SAW filter using effective permittivity and the coupling of modes model," *J. Phys. D, Appl. Phys.*, vol. 37, pp. 120–127, 2004.

[6] S. Ballandras, A. Reinhardt, V. Laude, A. Soufyane, S. Camou, W. Daniau, T. Pastureaud, W. Steichen, R. Lardat, M. Solal, and P. Ventura, "Simulations of surface acoustic wave devices built on stratified media using a mixed finite element/boundary integral formulation," *J. Appl. Phys.*, vol. 96, no. 12, pp. 7731–7741, 2004.

[7] T. Pastureaud, V. Laude, and S. Ballandras, "Stable scattering-matrix method for acoustic waves in piezoelectric multilayers," *Appl. Phys. Lett.*, vol. 80, pp. 2544–2546, 2002.

[8] R. T. Smith and F. S. Welsh, "Temperature dependence of elastic, piezoelectric, and dielectric constants of lithium tantalate and lithium niobate," *J. Appl. Opt.*, vol. 42, pp. 2219–2230, May 1971.

[9] Landolt-Börnstein, *Numerical Data and Functional Relationships in Science and Technology.* vol. 11, Group III, Crystal and Solid State Physics K. H. Hellwege and A. M. Hellwege, Eds. Berlin: Springer-Verlag, 1979.

[10] S. Ballandras, A. Reinhardt, V. Laude, A. Soufyane, S. Camou, W. Daniau, T. Pastureaud, W. Steichen, R. Lardat, M. Solal, and P. Ventura, "Simulations of surface acoustic wave devices built on stratified media using a mixed finite element/boundary integral formulation," *J. Appl. Phys.*, vol. 96, no. 12, pp. 7731–7741, 2004.

[11] B. Aspar, H. Moriceau, E. Jalaguier, C. Lagahe, A. Soubie, B. Biasse, A. M. Papon, A. Claverie, J. Grisolia, G. Benassayag, F. Letertre, O. Rayssac, T. Barge, C. Maleville, and B. Ghyselen, *J. Electron. Mater.*, vol. 30, no. 7, pp. 834–838, 2001.

[12] J. M. Hodé, J. Desbois, P. Dufilié, M. Solal, and P. Ventura, "SPUDT-based filters: Design, principles and optimization," in *Proc. IEEE Ultrason. Symp.*, 1995, pp. 39–47.

[13] M. Solal, T. Pastureaud, S. Ballandras, B. Aspar, B. Biasse, W. Daniau, W. Steichen, V. Laude, and A. Laëns, "Oriented lithium niobate layers transferred on 4″ (100) silicon wafer for RF SAW devices," in *Proc. IEEE Ultrason. Symp.*, 20022, pp. 128–131.

[14] T. Pastureaud, B. Biasse, B. Aspar, W. Daniau, W. Steichen, V. Laude, R. Lardat, A. Laens, J.-B. Briot, J.-M. Friedt, and S. Ballandras, "New theoretical and experimental results on high frequency surface acoustic waves excited on oriented $LiNbO_3$ single crystal layers transferred onto silicon," in *Proc. IEEE Ultrason. Symp.*, vol. 2, pp. 930–933, 2005.